Adaptive Interval Type-2 Fuzzy Controller Based Direct Torque Control of Permanent Magnet Synchronous Motor

Noureddine HENINI[1], Abdelhalim TLEMÇANI[1], Said BARKAT[2]
[1]*Laboratory of Research in Electrotechnic and Automatic, University of Médéa, 26000, Algeria*
[2]*Laboratory of Electrical Engineering, Faculty of Technology, University of M'sila, 28000, Algeria*
n.d.henini@gmail.com

***Abstract*—This paper develops an adaptive type-2 fuzzy logic controller for direct torque control of a permanent magnet synchronous motor. The type-2 fuzzy logic systems are used for modeling the unknown functions. The adaptive law proposed takes in consideration the compensation of reconstruction errors by adding a sliding mode term. This term ensures the stability and the robustness of the control system regardless the internal and external disturbances. The stability of closed-loop system was verified using Lyapunov's stability theorem. Moreover, the proposed control scheme guarantees that all involved signals are bounded. The effectiveness and the feasibility of the proposed control method are demonstrated by extensive presentation and discussion of simulation results.**

***Index Terms*—adaptive control, fuzzy systems, measurement uncertainty, permanent magnet motor, torque control.**

I. Introduction

Permanent magnet synchronous motors (PMSM) are efficiently used in industrial applications. They have relatively higher power density, high torque/inertia ratio, and slight rotor losses and easy to control. These qualities make PMSM a competitive choice in various high-performance, robotic, and servo applications.

There are two types of drive system used for PMSM: vector and direct torque control (DTC) drives. The direct torque control has many advantages compared with the vector control. Most importantly, the position signal and the current controllers used in vector control are not necessary in PMSM DTC drive. It is carried out using only a switching table and hysteresis controllers. In the classical DTC, the output of hysteresis comparator for flux linkage can be 0 or 1, and for electromagnet torque it can be 1, 0, -1 to reduce torque ripple, by using three-level hysteresis torque controller. Thus, the results cannot distinguish error size and the inverter switching frequency cannot be controlled [1-2]. In addition, the voltage vector selected cannot, in most cases, compensate flux linkage error and electromagnetic torque error. To overcome these problems, various methods have been proposed [3-6]. Most of above-mentioned difficulties were eliminated by using PI controllers with space vector modulation (SVM). However, the PI controller may not give satisfying performance under a non-linearity of PMSM, parameter variations and external disturbances. Thus, the development of a more robust adaptive controller for PMSM drive is required.

In recent years, the adaptive control of PMSM with unknown dynamics using type-1 fuzzy logic systems (T1FLSs) has interested many researchers [7-12]. These systems are able to capture effectively the system nonlinearities but not the system uncertainties. The type-2 fuzzy logic systems (T2FLSs) are more effective approach for handling uncertainties. It is used successfully in different applications such as: control [13-16], medical applications [17], noise tolerance analysis [18], DC-DC converters [19], intelligent transportation systems [20], robotic systems [21, 22], linear ultrasonic motors [23], motion control systems [24-25], electrical drive [26-28].

In this paper, an adaptive type-2 fuzzy control technique is proposed for a DTC of PMSM. The Lyapunov method is used to obtain the adaptive laws of fuzzy systems, reconstruction error bounds and robust terms. Furthermore, the space vector modulation technique is used to control the inverter. All this makes it possible not only to have a DTC operating at a fixed switching frequency but also to take into account the nonlinearity and uncertainty of the system, which makes our control method more robust than the others proposed in the literature.

This paper is organized as follows: Section II discusses the PMSM motor model, and section III introduces the problem statement. Section IV describes the type-2 fuzzy logic system. The proposed method is developed in section V. In section VI, the performance of the proposed scheme is evaluated. As for section VII, it compares the proposed method with the literature. Finally, a general conclusion is drawn.

II. Mathematical Model of PMSM

The PMSM model, in the synchronous d-q reference frame, without consideration of damping effect, saturation and considering sinusoidal distribution of stator winding, is represented as follows [9]:

$$\begin{cases} v_d = R_s i_d + L_d \dfrac{di_d}{dt} - pL_q \Omega i_q \\ v_q = R_s i_q + L_q \dfrac{di_q}{dt} + pL_d \Omega i_d + p\Omega\Phi_f \\ J\dfrac{d\Omega}{dt} = T_{em} - T_r - F_c\Omega \\ T_{em} = \dfrac{3}{2} p\left(\Phi_f i_q + \left(L_d - L_q\right) i_d i_q\right) \end{cases} \tag{1}$$

where:

v_d, v_q : stator voltage in d-q-axis;

Digital Object Identifier 10.4316/AECE.2021.02002

1582-7445 © 2021 AECE

i_d, i_q : stator current in d-q-axis;

L_d, L_q : stator inductance in d-q-axis;

R_s : stator resistance;

p : number of pole pairs;

Ω : mechanical speed;

Φ_f : flux created by the rotor magnets;

T_{em}, T_r : electromagnetic torque and load torque;

F_c : viscous friction coefficient;

J : total moment of inertia of the motor and load.

In order to control directly and independently the flux and the torque, the PMSM model is expressed in the stator flux reference frame *x-y* by using the following transformation:

$$T_{dq/xy} = \begin{pmatrix} \cos\delta & \sin\delta \\ -\sin\delta & \cos\delta \end{pmatrix} \tag{2}$$

The voltage components in *x-y* frame are as follows:

$$\begin{cases} v_x = R_s i_x - \omega_s L_d i_y + L_d \dfrac{di_x}{dt} + p\Omega\Phi_f \sin\delta \\ v_y = R_s i_y + \omega_s L_q i_x + L_q \dfrac{di_y}{dt} + p\Omega\Phi_f \cos\delta \end{cases} \tag{3}$$

where:

ω_s : rotating speed of stator flux linkage

δ: angle between rotor and stator flux linkage.

v_x, v_y : stator voltage components in x-y frame;

i_x, i_y : stator current components in *x-y* frame;

The stator flux linkage and the electromagnetic torque are given by:

$$\begin{cases} \phi_x = \phi_s = L_d i_x + \Phi_f \cos\delta \\ \phi_y = 0 = L_d i_y - \Phi_f \sin\delta \\ T_{em} = p\phi_s i_y \end{cases} \tag{4}$$

ϕ_x, ϕ_y : stator flux components in *x-y* frame;

ϕ_s : stator flux magnitude;

From (3) and (4), PMSM model can be written as follow:

$$\begin{cases} \dfrac{d\phi_s}{dt} = f_1 + b_1 v_x \\ \dfrac{dT_{em}}{dt} = f_2 + b_2 v_y \\ \dfrac{d\Omega}{dt} = f_3 + b_3 T_e \end{cases} \tag{5}$$

where:

$$\begin{cases} f_1 = -\dfrac{R_s}{L_d}\left(\phi_s - \Phi_f \cos\delta\right) \\ f_2 = -\dfrac{p\phi_s}{L_d}\left(R_s i_y + \omega_s\phi_s + \left(\omega_s - p\Omega\right)\Phi_f \cos\delta\right) - p i_y \dot{\phi}_s \\ f_3 = -\dfrac{1}{j}\left(T_r + F_c\Omega\right) \\ b_1 = 1 \\ b_2 = \dfrac{p\phi_s}{L_d} \\ b_3 = \dfrac{1}{j} \end{cases} \tag{6}$$

III. Problem Statement

We aim to build a DTC adaptive type-2 fuzzy control for a PMSM in order to reduce the torque ripple and to impose the switching frequency. The control problem is to force system (5) to follow a given bounded reference signals.

PMSM model can be written as follow:

$$\begin{cases} \dfrac{d\phi_s}{dt} = f_1 + b_1 v_x \\ \dfrac{dT_{em}}{dt} = f_2 + b_2 v_y \\ \dfrac{d\Omega}{dt} = f_3 + b_3 T_e \end{cases} \tag{7}$$

Let us first consider the ideal case where the functions f_1, f_2 and f_3 and the constants b_2 and b_3 are well known. This is a necessary step to take when the control objective cannot be met in the case of known PMSM model; it is not useful in the case of unknown PMSM model.

Let us consider the Lyapunov-like function:

$$V = \frac{1}{2}\left(e_1 + e_2 + e_3\right) \tag{8}$$

where: $$\begin{cases} e_1 = \phi_s^* - \phi_s \\ e_2 = T_e^* - T_e \\ e_3 = \Omega^* - \Omega \end{cases} \tag{9}$$

Its time derivative is given by:

$$\dot{V} = \dot{e}_1 e_1 + \dot{e}_2 e_2 + \dot{e}_3 e_3 \tag{10}$$

The derivative of the errors (8) becomes:

$$\begin{cases} \dot{e}_1 = \dfrac{df^*_s}{dt} - f_1 - b_1 v_x \\ \dot{e}_2 = \dfrac{dT^*_{em}}{dt} - f_2 - b_2 v_y \\ \dot{e}_3 = \dfrac{d\Omega^*}{dt} - f_3 - b_3 T_e \end{cases} \tag{11}$$

If the ideal control laws v_x^*, v_y^* and T_{em}^* are forced as:

$$\begin{cases} v_x^* = \dfrac{1}{b_1}\left(-f_1 + \dfrac{df_s^*}{dt} + k_1 e_1\right) \\ v_y^* = \dfrac{1}{b_2}\left(-f_2 + \dfrac{dT_{em}^*}{dt} + k_2 e_2\right) \\ T_{em}^* = \dfrac{1}{b_3}\left(-f_3 + \dfrac{d\Omega^*}{dt} + k_3 e_3\right) \end{cases} \tag{12}$$

where: $k_1, k_2\ k_3 > 0$

Then, $\dot{V}$ fulfils the inequality:

$$\dot{V} = -k_1 e_1^2 - k_2 e_2^2 - k_3 e_3^2 < 0 \tag{13}$$

Relation (12), mean that e_1, e_2 and e_3 converge asymptotically to zero. Therefore, the control laws (12) can drive ideally the system.

However, the functions f_1, f_2 and f_3 and the constants b_2 and b_3 are actually unknown, so we cannot use them to construct the equivalent ideal control (12). In this context, we propose to replace the unknown terms by a type-2 fuzzy system.

IV. Type-2 Fuzzy Logic System Design

Fig. 1 depicts the structure of T2FLS. It is quite similar to the T1FLS. The major difference is that the fuzzy sets are type-2 and in order to convert the output of the fuzzy inference engine into a type-1 fuzzy set, we must use a type-reducer subsystem. This type-reduced set is defuzzified to obtain the crisp output.

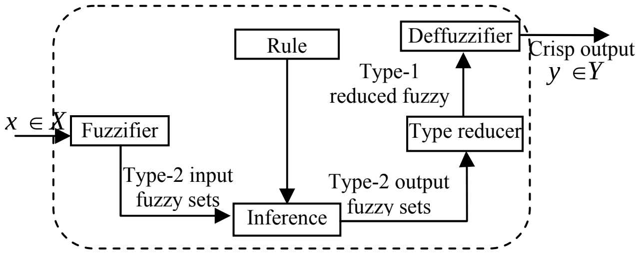

Figure 1. Structure of a T2FLS

Consider a T2FLS having:

n inputs, $x = \left\lceil x_{1,\dots,}x_n \right\rceil \in X_1 \times \dots \times X_n$;

one output $y \in Y$;

and M rules, where the i^{th} rule has the form:

$$R^i : IF\ x_1\ is\ \tilde{F}_1^i\ and\ \dots and\ x_n\ is\ \tilde{F}_n^i\ THEN \quad y^i = C^i\ ;\ i = 1,..,M \tag{14}$$

with:

$\tilde{F}_1^i, \tilde{F}_2^i, \dots, \tilde{F}_n^i$ are the antecedent linguistic terms. They are modelled by the interval type-2 Gaussian fuzzy sets (Fig. 2):

y is the output of ith rule R^i ;

C^i is the consequent parameter.

In Fig. 2, the footprint of uncertainty (FOU) can be represented as a bounded interval in terms of the upper membership function $\bar{\mu}_{\tilde{F}_j^i}(x_j)$ and the lower membership function $\underline{\mu}_{\tilde{F}_j^i}(x_j)$, where:

$$\bar{\mu}_{\tilde{F}_j^i}(x_j) = \exp\left[-\frac{1}{2}\left(\frac{x_j - m_j}{\sigma_j}\right)^2 \right] \equiv N(m_j, \sigma_j, x_j) \quad \text{and} \quad \underline{\mu}_{\tilde{F}_j^i}(x_j) = 0.8\bar{\mu}_{\tilde{F}_j^i}(x_j) \tag{15}$$

m_j and σ_j are respectively the mean and the standard deviation of Gaussian primary MF of the type-2 fuzzy set $\tilde{F}_j^i$.

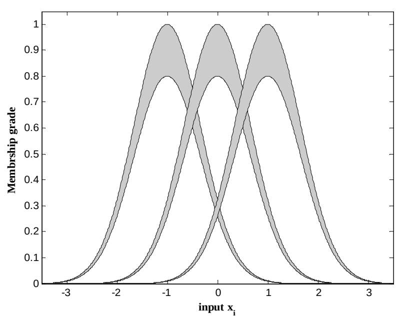

Figure 2. Interval type-2 Gaussian membership functions for antecedents sets

The firing interval $[\underline{f}^i, \bar{f}^i]$ of the i^{th} rule is an interval type-1 set; where $\underline{f}^i$ and $\bar{f}^i$ are determined as follows:

$$\underline{f}^i = \underline{\mu}_{\tilde{F}_1^i}(x_1) * \underline{\mu}_{\tilde{F}_2^i}(x_2) * \dots * \underline{\mu}_{\tilde{F}_n^i}(x_n) \tag{16}$$

$$\bar{f}^i = \bar{\mu}_{\tilde{F}_1^i}(x_1) * \bar{\mu}_{\tilde{F}_2^i}(x_2) * \dots * \bar{\mu}_{\tilde{F}_n^i}(x_n) \tag{17}$$

with $\underline{\mu}_{\tilde{F}_j^i}(x_j)$ and $\bar{\mu}_{\tilde{F}_j^i}(x_j)$ represent the membership value of the lower and the upper membership functions of the crisp input x_j to the type-2 fuzzy set $\tilde{F}_j^i$ in the i^{th} rule.

The final output can be expressed as [29]:

$$Y = [y_l, y_r] = \int_{\theta^1} \dots \int_{\theta^M} \dots \int_{f^1} \dots \int_{f^M} 1 \Bigg/ \frac{\sum_{i=1}^{M} f^i \theta^i}{\sum_{i=1}^{M} f^i} \tag{18}$$

The output Y is an interval type-1 set; its two endpoints y_l and y_r can be represented as follows:

$$y_l = \frac{\sum_{i=1}^{M} f_l^i \theta^i}{\sum_{i=1}^{M} f_l^i} = \sum_{i=1}^{M} W_l^i(x)\theta^i = W_l^T(x)\theta \tag{19}$$

and:

$$y_r = \frac{\sum_{i=1}^{M} f_r^i \theta^i}{\sum_{i=1}^{M} f_r^i} = \sum_{i=1}^{M} W_r^i(x)\theta^i = W_r^T(x)\theta \tag{20}$$

where:

f_l^i and f_r^i represent the firing strength membership grades contributing to the left-most-point y_l and the right-most-point y_r respectively.

$\theta = \left[\theta^1, \dots, \theta^M\right]$. With: θ^i are considered as type-1 centroids of the consequent sets.

The fuzzy basis functions $W_l^i(x) = f_l^i \Big/ \sum_{i=1}^{M} f_l^i$ and $W_r^i(x) = f_r^i \Big/ \sum_{i=1}^{M} f_r^i$ are the components of left and right FBF vectors defined by: $W_l^T(x) = \left[W_l^1(x), \dots, W_l^M(x)\right]$ and $W_r^T(x) = \left[W_r^1(x), \dots, W_r^M(x)\right]$.

In order to compute Y, we need to compute y_l and y_r. This can be achieved using the iterative procedure given in [30]:

Step 1: Compute y_r in (20) by initially setting $f_r^i = (\underline{f}^i + \bar{f}^i)/2$, for $i = 1,2,\dots,M$ where $\underline{f}^i$ and $\bar{f}^i$ have been computed using (15) and (16) respectively, and let $y_r{}' = y_r$.

Step 2: Find $k\left(1 \le k \le M-1\right)$ such that $\theta^k \le y_r^{'} \le \theta^{k+1}$.

Step 3: Compute y_r in (20) with $f_r^i = \underline{f}^i$ for $i \le k$ and $f_r^i = \bar{f}^i$ for $i > k$, then set $y_r^{''} = y_r$.

Step 4: If $y_r^{''} \ne y_r^{'}$, then go to step 5. If $y_r^{''} = y_r^{'}$ then set $y_r = y_r^{''}$ and go to step 6.

Step 5: Set $y_r^{'} = y_r^{''}$ and return to *step 2*.

Step 6: End.

The procedure for computing y_l is very similar; only two changes need to be made: In *step 2*, we need to find ($1 \le k' \le M-1$) such that $\theta^{k'} \le y_l' \le \theta^{k'+1}$ and in *step 3*, let $f_l^i = \overline{f}^i$ for $i \le k'$ and $f_l^i = \underline{f}^i$ for $i > k'$.

The crisp output can be obtained by means of the average value of y_l and y_r. Hence, the defuzzified crisp output becomes:

$$y = \frac{W_l^T(x) + W_r^T(x)}{2}\theta = W^T(x)\theta \tag{21}$$

V. CONTROL SYNTHESIS AND STABILITY ANALYSIS

The approximation propriety of the fuzzy logic system defined in (21) allows us to assume that the nonlinear functions given in (11) can be reconstructed by type-2 Sugeno-Tagaki fuzzy system as follows:

$$\begin{cases} v_x^* = W_1^T(\phi_s)\,\theta_1 + \varepsilon_1(\phi_s) \\ v_y^* = W_2^T(T_e)\,\theta_2 + \varepsilon_2(T_{em}) \\ T_{em}^* = W_3^T(\Omega)\,\theta_3 + \varepsilon_3(\Omega) \end{cases} \tag{22}$$

The vectors parameters θ_i (i =1,2,3) are the best parameters, and ε_i are the unavoidable reconstruction errors. These reconstruction errors are assumed bounded:

$$\begin{cases} |\varepsilon_1(\phi_s)| \le \overline{\varepsilon}_1 \\ |\varepsilon_2(T_{em})| \le \overline{\varepsilon}_2 \\ |\varepsilon_3(\Omega)| \le \overline{\varepsilon}_3 \end{cases} \tag{23}$$

where: $\overline{\varepsilon}_i$ are unknown positive parameters.

Moreover, the estimation of ideal control law can be written under the form:

$$\begin{cases} \hat{v}_x = W_1^T(\phi_s)\,\hat{\theta}_1 \\ \hat{v}_y = W_2^T(T_e)\,\hat{\theta}_2 \\ \hat{T}_{em} = W_3^T(\Omega)\,\hat{\theta}_3 \end{cases} \tag{24}$$

where: $\hat{\theta}_i$ are the estimation of the parameters θ_i.

By using the equations (22) and (24), it follows that:

$$\begin{cases} v_x^* - \hat{v}_x = W_1^T(\phi_s)\,\tilde{\theta}_1 + \varepsilon_1(\phi_s) \\ v_y^* - \hat{v}_y = W_2^T(T_{em})\,\tilde{\theta}_2 + \varepsilon_2(T_{em}) \\ T_{em}^* - \hat{T}_{em} = W_3^T(\Omega)\,\tilde{\theta}_3 + \varepsilon_3(\Omega) \end{cases} \tag{25}$$

where: $\tilde{\theta}_i = \theta_i - \hat{\theta}_i$ is vector parametric error.

By using the estimated functions, the control laws become:

$$\begin{cases} \hat{v}_x^* = \hat{v}_x + v_{xa} \\ \hat{v}_y^* = \hat{v}_y + v_{ya} \\ \hat{T}_{em}^* = \hat{T}_{em} + T_{ema} \end{cases} \tag{26}$$

where:

v_{xa}, v_{ya} and T_{ema} are sliding mode terms, they are introduced in order to compensate the effects of the reconstruction errors. These robust control terms are defined as follows:

$$\begin{cases} v_{xa} = \hat{\overline{\varepsilon}}_1\, sign(e_1) \\ v_{ya} = \hat{\overline{\varepsilon}}_2\, sign(e_2) \\ T_{ema} = \hat{\overline{\varepsilon}}_3\, sign(e_3) \end{cases} \tag{27}$$

The bounds of the reconstruction errors are estimated by the laws:

$$\begin{cases} \dot{\hat{\overline{\varepsilon}}}_1 = \eta_1 |e_1| \\ \dot{\hat{\overline{\varepsilon}}}_2 = \eta_2 |e_2| \\ \dot{\hat{\overline{\varepsilon}}}_3 = \eta_3 |e_3| \end{cases} \tag{28}$$

The parameters of the T2FLS are adjusted by the following laws:

$$\begin{cases} \dot{\hat{\theta}}_1 = \gamma_1 W_1^T(\phi_s)\, e_1 \\ \dot{\hat{\theta}}_2 = \gamma_2 W_2^T(T_{em})\, e_2 \\ \dot{\hat{\theta}}_3 = \gamma_3 W_3^T(\Omega)\, e_3 \end{cases} \tag{29}$$

where: η_i and γ_i are positives constants.

By using the equations (11) and (22), we can write:

$$\begin{cases} -f_1 = -\left(\frac{d\phi_s^*}{dt} + k_1 e_1\right) + b_1\left(W_1^T(\phi_s)\,\theta_1 + \varepsilon_1(\phi_s)\right) \\ -f_2 = -\left(\frac{dT_{em}^*}{dt} + k_2 e_2\right) + b_2\left(W_2^T(T_{em})\,\theta_2 + \varepsilon_2(T_{em})\right) \\ -f_3 = -\left(\frac{d\Omega^*}{dt} + k_3 e_3\right) + b_3\left(W_3^T(\Omega)\,\theta_3 + \varepsilon_3(\Omega)\right) \end{cases} \tag{30}$$

By substituting the equations (30), (25), (26) and (22) in the equation (10), the dynamic errors are:

$$\begin{cases} \dot{e}_1 = -k_1 e_1 + b_1\left(W_1^T(\phi_s)\,\tilde{\theta}_1 + \varepsilon_1(\phi_s) - v_{xa}\right) \\ \dot{e}_2 = -k_2 e_2 + b_2\left(W_2^T(T_{em})\,\tilde{\theta}_2 + \varepsilon_2(T_{em}) - v_{ya}\right) \\ \dot{e}_3 = -k_3 e_3 + b_3\left(W_3^T(\Omega)\,\tilde{\theta}_3 + \varepsilon_3(\Omega) - T_{ema}\right) \end{cases} \tag{31}$$

Let us consider Lyapunov-like function:

$$V = V_1 + V_2 + V_3 \tag{32}$$

$$\text{where: } \begin{cases} V_1 = \frac{1}{2b_1}e_1^2 + \frac{1}{2\gamma_1}\tilde{\theta}_1^T\tilde{\theta}_1 + \frac{1}{2\eta_1}\tilde{\overline{\varepsilon}}_1^2 \\ V_2 = \frac{1}{2b_2}e_2^2 + \frac{1}{2\gamma_2}\tilde{\theta}_2^T\tilde{\theta}_2 + \frac{1}{2\eta_2}\tilde{\overline{\varepsilon}}_2^2 \\ V_3 = \frac{1}{2b_3}e_3^2 + \frac{1}{2\gamma_3}\tilde{\theta}_3^T\tilde{\theta}_3 + \frac{1}{2\eta_3}\tilde{\overline{\varepsilon}}_3^2 \end{cases} \tag{33}$$

with: $\tilde{\overline{\varepsilon}}_i = \overline{\varepsilon}_i - \hat{\overline{\varepsilon}}_i$.

The time derivative of each function V_i ($i = 1,2,3$) is given by:

$$\begin{cases} \dot{V}_1 = \frac{1}{b_1}e_1\dot{e}_1 - \frac{1}{\gamma_1}\tilde{\theta}_1^T\dot{\hat{\theta}}_1 - \frac{1}{\eta_1}\tilde{\overline{\varepsilon}}_1\dot{\hat{\overline{\varepsilon}}}_1 \\ \dot{V}_2 = \frac{1}{b_2}e_2\dot{e}_2 - \frac{1}{\gamma_2}\tilde{\theta}_2^T\dot{\hat{\theta}}_2 - \frac{1}{\eta_2}\tilde{\overline{\varepsilon}}_2\dot{\hat{\overline{\varepsilon}}}_2 \\ \dot{V}_3 = \frac{1}{b_3}e_3\dot{e}_3 - \frac{1}{\gamma_3}\tilde{\theta}_3^T\dot{\hat{\theta}}_3 - \frac{1}{\eta_3}\tilde{\overline{\varepsilon}}_3\dot{\hat{\overline{\varepsilon}}}_3 \end{cases} \tag{34}$$

By exploiting (29) and (31), relation (34) is reduced to:

$$\begin{cases} \dot{V}_1 = -\dfrac{k_1}{b_1}e_1^2 + \varepsilon_1(\phi_s)e_1 - v_{xa}e_1 - \dfrac{1}{\eta_1}\tilde{\tilde{\varepsilon}}_1\dot{\hat{\varepsilon}}_1 \\ \dot{V}_2 = -\dfrac{k_2}{b_2}e_2^2 + \varepsilon_2(T_{em})e_2 - v_{ya}e_2 - \dfrac{1}{\eta_2}\tilde{\tilde{\varepsilon}}_2\dot{\hat{\varepsilon}}_2 \\ \dot{V}_3 = -\dfrac{k_3}{b_3}e_3^2 + \varepsilon_3(w)e_3 - T_{ema}e_3 - \dfrac{1}{\eta_3}\tilde{\tilde{\varepsilon}}_3\dot{\hat{\varepsilon}}_3 \end{cases} \quad (35)$$

The substitution of (27) in (35) leads to:

$$\begin{cases} \dot{V}_1 = -\dfrac{k_1}{b_1}e_1^2 + \varepsilon_1(\phi_s)e_1 - \hat{\hat{\varepsilon}}_1|e_1| - \dfrac{1}{\eta_1}\tilde{\tilde{\varepsilon}}_1\dot{\hat{\varepsilon}}_1 \\ \dot{V}_2 = -\dfrac{k_2}{b_2}e_2^2 + \varepsilon_2(T_{em})e_2 - \hat{\hat{\varepsilon}}_2|e_2| - \dfrac{1}{\eta_2}\tilde{\tilde{\varepsilon}}_2\dot{\hat{\varepsilon}}_2 \\ \dot{V}_3 = -\dfrac{k_3}{b_3}e_3^2 + \varepsilon_3(\Omega)e_3 - \hat{\hat{\varepsilon}}_3|e_3| - \dfrac{1}{\eta_3}\tilde{\tilde{\varepsilon}}_3\dot{\hat{\varepsilon}}_3 \end{cases} \quad (36)$$

The conditions (23) applied to relations (36) make that $\dot{V}_i$ ($i = 1,2,3$) achieve always the inequalities:

$$\begin{cases} \dot{V}_1 \le -\dfrac{k_1}{b_1}e_1^2 + \tilde{\tilde{\varepsilon}}_1|e_1| - \dfrac{1}{\eta_1}\tilde{\tilde{\varepsilon}}_1\dot{\hat{\varepsilon}}_1 \\ \dot{V}_2 \le -\dfrac{k_2}{b_2}e_2^2 + \tilde{\tilde{\varepsilon}}_2|e_2| - \dfrac{1}{\eta_2}\tilde{\tilde{\varepsilon}}_2\dot{\hat{\varepsilon}}_2 \\ \dot{V}_3 \le -\dfrac{k_3}{b_3}e_3^2 + \tilde{\tilde{\varepsilon}}_3|e_3| - \dfrac{1}{\eta_3}\tilde{\tilde{\varepsilon}}_3\dot{\hat{\varepsilon}}_3 \end{cases} \quad (37)$$

Use the update laws (28) allow reducing inequalities (37) as:

$$\begin{cases} \dot{V}_1 \le -\dfrac{k_1}{b_1}e_1^2 \\ \dot{V}_2 \le -\dfrac{k_2}{b_2}e_2^2 \\ \dot{V}_3 \le -\dfrac{k_3}{b_3}e_3^2 \end{cases} \quad (38)$$

From the inequalities (38), we conclude that $\dot{V}_1$, $\dot{V}_2$ and $\dot{V}_3$ are negative definite functions. This implies that the parameters $\tilde{\theta}_i$ and $\tilde{\tilde{\varepsilon}}_i$ ($i = 1,2,3$) are bounded which implies that the speed (Ω), stator flux (f_s) and torque (T_{em}) are bounded for all $t \ge 0$. From the relations (26) to (28), it is obvious that the control signals are bounded. Since V_1, V_2 and V_3 are positive definite and none increasing function therefore the variables e_1, e_2 and e_3 converge at least asymptotically toward zero.

VI. Simulation Results

The proposed scheme of the adaptive interval type-2 fuzzy controller based DTC of PMSM is shown in Fig. 3.

The control coefficients and the parameters of PMSM values of are given in the appendix A and B respectively.

The parameters η_i and γ_i ($i = 1,2,3$) control both the convergence speed of the fuzzy systems' parameters and the gains of the robust terms. We chose small parameters in order to minimize the convergence speed which impacts the control quality. After several trials, we reached satisfactory results.

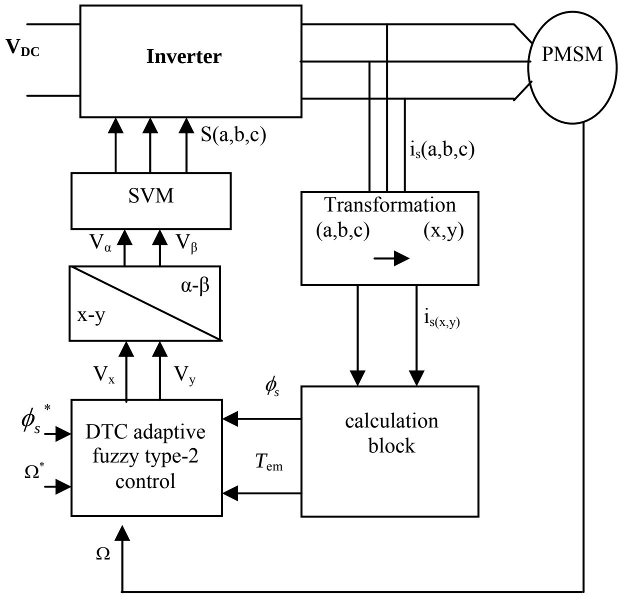

Figure 3. Scheme of the adaptive DTC of the PMSM based on type-2 fuzzy logic

Five tests are done for performance evaluation of the proposed approach:

1. *Linear reference speed tracking*:

The first test deals with reference speed change from 0 to $\Omega_n/2$ with a slope of $\Omega_n/0.4$ then from $\Omega_n/2$ to Ω_n with a slope of $\Omega_n/0.4$ and finally from Ω_n to $-\Omega_n$ with a slope of $-\Omega_n/0.2$, and maintaining the stator flux f_s^* to 0.314 Wb.

2. *Sinusoidal reference speed tracking*:

The second test is done with sinusoidal trajectory as a desired rotor speed Ω_{ref} ($\Omega_{ref} = \Omega_n \sin\left(\dfrac{\pi}{2}t\right)$ rad/s) and f_s^* is set to 0.314 Wb as a desired stator flux.

3. *Load torque disturbances*:

The third test aims to evaluate the robustness of the proposed approach to the external disturbances. Hence, the nominal load torque is applied at 2s.

4. *Parametric variations*:

Internal disturbances or parametric variations were studied in the fourth test. Thus, at t = 1.5s, we proceeded as follows:

- Increasing the stator resistances and the moment of inertia by 100%;
- Decreasing stator inductances by 50%;
- Reducing of the inductor flux by 5%.

5. *Field weakening operation*:

The last test examines the PMSM behavior in the flux weakening region. An increase in the rotor speed above 100% at t = 2s is applied.

Fig. 4, Fig. 5, Fig. 6, Fig. 7 and Fig. 8 show the responses of the PMSM for the five tests discussed above. For each test, the results show that the stator flux and the speed follow the desired references accurately. Also the disturbance rejection is fast and the stator flux draws a circular trajectory. In addition, the speed and stator flux tracking errors remain satisfactory even for the parametric variations.

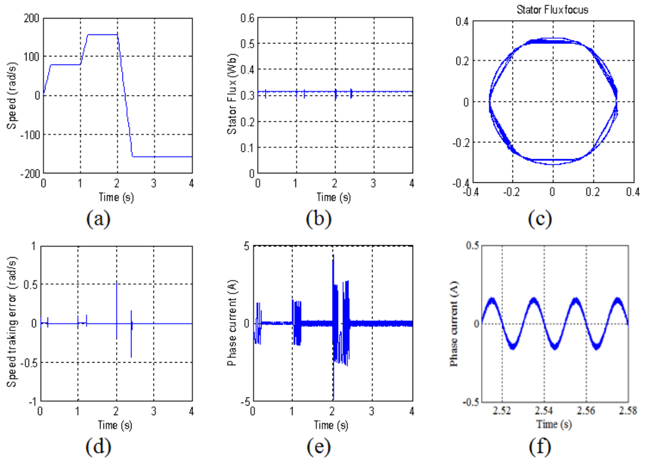

Figure 4. Simulation results for evaluating controller speed tracking: (a) Rotor speed, (b) Stator flux, (c) Stator flux focus, (d) Speed tracking error, (e) Phase current, (f) Phase current zoom

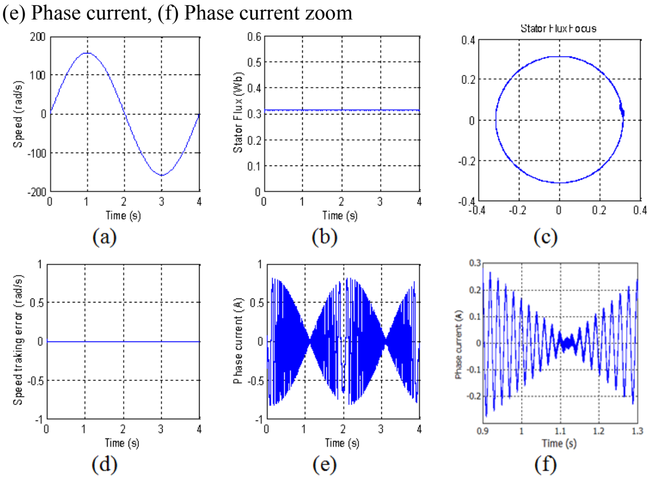

Figure 5. Simulation results for evaluating controller speed tracking in case of a sinusoidal trajectory of rotor speed reference: (a) Rotor speed, (b) Stator flux, (c) Stator flux focus, (d) Speed tracking error, (e) Phase current, (f) Phase current zoom

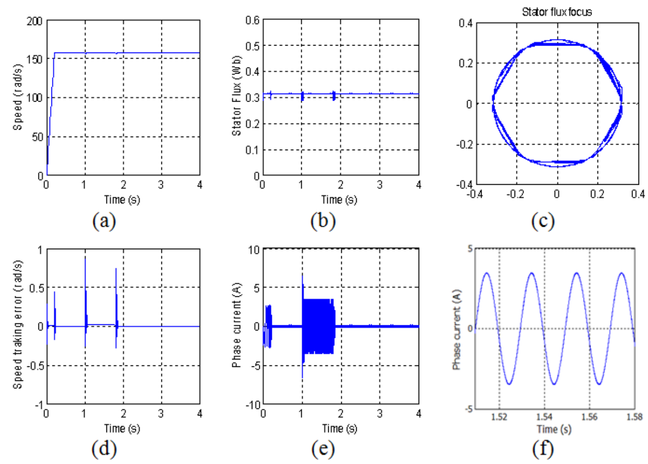

Figure 6. DTC robustness against load torque variation: (a) Rotor speed, (b) Stator flux, (c) Stator flux focus, (d) Speed tracking error, (e) Phase current, (f) Phase current zoom

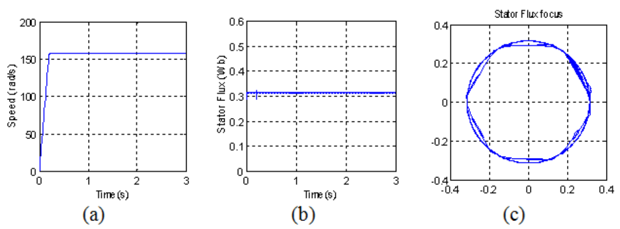

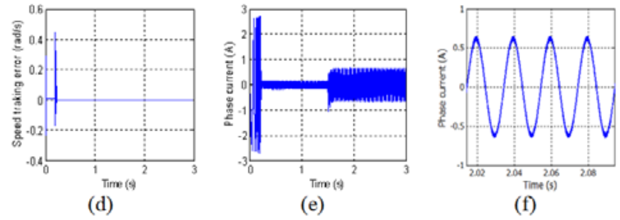

Figure 7. DTC against parametric variations: (a) Rotor speed, (b) Stator flux, (c) Stator flux focus, (d) Speed tracking error, (e) Phase current, (f) Phase current zoom

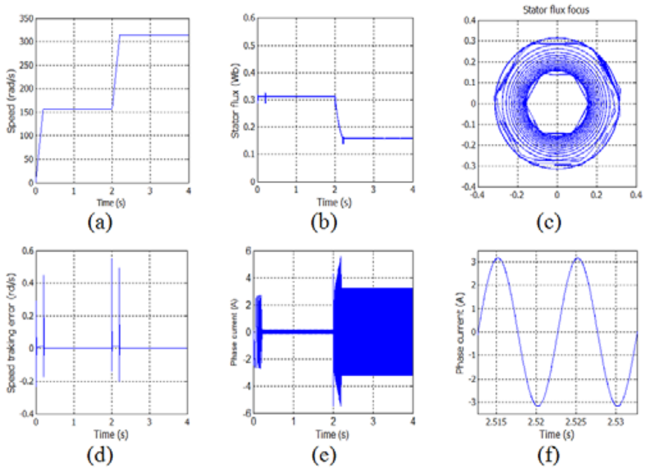

Figure 8. Simulation results for evaluating the proposed DTC during field weakening operation: (a) Rotor speed, (b) Stator flux, (c) Stator flux focus, (d) Speed tracking error, (e) Phase current, (f) Phase current zoom

VII. Comparative Analysis of the Results

The Fig. 9, Fig. 10, Fig. 11 and Fig. 12 present the torque response for the four tests discussed in the section VI, in order to compare the torque ripples between the conventional lookup table based DTC (with three-level hysteresis torque controller) and the proposed DTC. In the classical DTC, the hysteresis controller bandwidths were chosen as follows:

0.1 N.m for the torque and 0.001 Wb for the flux.

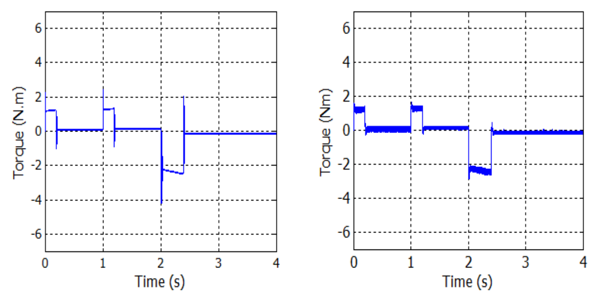

(a) Proposed DTC (b) Classical DTC

Figure 9. Torque response under conditions of first test

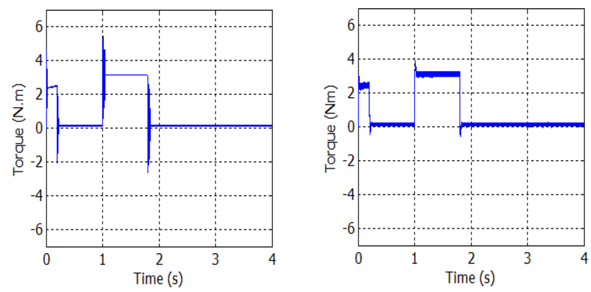

(a) Proposed DTC (b) Classical DTC

Figure 10. Torque response following the application of the second test

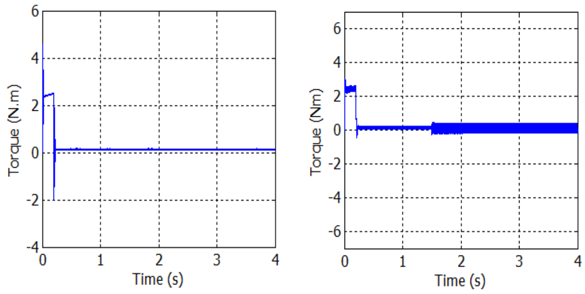

(a) Proposed DTC (b) Classical DTC

Figure 11. Torque response under conditions of the third test

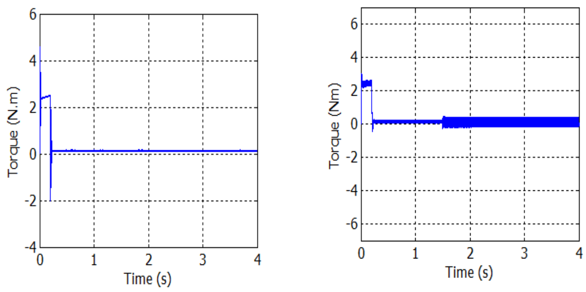

(a) Proposed DTC (b) Classical DTC

Figure 12. Torque response under conditions of the fourth test

As illustrated, the torque ripple of the proposed DTC is significantly inferior to that of classical DTC using PI speed controller.

Moreover, our proposed approach has better performances than that in the literature. Here are some examples that prove our point of view.

In [31], a fuzzy logic controller is designed by the authors; it is linked to direct torque control strategy for a PMSM. A stator flux angle mapping technique is suggested to significantly reduce the rule base so that the fuzzy reasoning speed increases. Besides, in a given sampling period, the inverter switch time cannot be controlled under hysteresis comparator leading to inconstant inverter switch frequency which may cause mechanical excitation (and noise) or acoustic resonances. In the proposed approach, however, the inverter switching frequency is constant.

In [32], to investigate the stability analysis of interval type-2 Takagi–Sugeno fuzzy logic control systems, the classical approach needed to make some assumptions regarding membership functions to derive stability conditions. This limits using the approach to just specific situations. It is worth mentioning that the old approach did not use any systematic method to identify the required membership function parameters to fix the inequalities of those assumptions. The old model structure produces linear matrix inequalities that are difficult to simplify or evaluate in order to ensure stability criteria [33]. Our approach makes realistic assumptions and uses type 2 fuzzy systems for approximation of the nonlinear functions and to ensure the stability and the robustness of the control structure opposite to the reconstruction errors and the interconnection effects; between the subsystems, we introduced robust sliding terms. The proposed control law is always stable and well defined.

Furthermore, in order to perform the feedback control of the PMSM, several sensors are required. However, sensor readings are often noisy. In order to simulate the influence of uncertainty in the speed measurement, a random noise with normal distribution is added to the measured speed.

Three performances criteria are used to compare between DTC based on adaptive type-1 and type-2 fuzzy logic controllers:

- Integral of square error (ISE);
- Integral of the absolute value of the error (IAE);
- Integral of the time multiplied by the absolute value of the error (ITAE).

During 3 seconds of system operation, the obtained values are recapitulated in Table I.

TABLE I. PERFORMANCE CRITERIA VALUES FOR DTC BASED ON ADAPTIVE TYPE-1 AND TYPE-2 FUZZY LOGIC CONTROLLERS

		Modeling uncertainty	**Measurement uncertainty**	**Modeling and measurement uncertainties**
ISE	Speed DTCAT1FLC	98.3	626650	614980
	Speed DTCAT2FLC	98.3	606600	605000
IAE	Speed DTCAT1FLC	1799	403260	399430
	Speed DTCAT2FLC	1799	396850	396130
ITAE	Speed DTCAT1FLC	588.8	407690	402870
	Speed DTCAT2FLC	588.8	399840	397970

The different criteria values for the modeling uncertainty are similar, for the two controller studied. For that, DTC adaptive type-1 fuzzy controller is recommended when the uncertainty in modeling must be handled, because their implementation is easier. However, the criteria values of measurement uncertainty for the adaptive type-2 fuzzy controller are lower. This makes it the better candidate when the measurement uncertainty is targeted.

VIII. CONCLUSION

In this work, an adaptive DTC based on type-2 fuzzy systems for PMSM has investigated. The control law developed incorporates an adaptive sliding term which can compensate the reconstruction errors regardless of internal or external disturbances. The obtained simulation results show that this law can be ensures satisfactory errors in term of references tracking. Moreover, the tracking errors are not strongly influenced by the variations of machine parameters speed measurement uncertainty and external disturbances. The simplicity of the proposed control law allows him easy to implement in real-time control systems.

APPENDIX A

TABLE II. CONTROL COEFFICIENTS

Symbol	**Value**
η_1	0.01
γ_1	0.01
η_2	0.01
γ_2	0.01
η_3	0.01
γ_3	0.01

APPENDIX B

The PMSM is characterized by: $L_d = L_q = 0.05H$, $R_s = 1.5\Omega$, $j = 0.003\ kgm^2$, $F_c = 0.0009\ N.m.s/rd$, $\Phi_f = 0.314\ Wb$, $\Omega_n = 157.0796 rd/s$.

REFERENCES

[1] L. Zhong, M. F. Rahman, W. Y. Hu, K.W. Lim, "Analysis of direct torque control in permanent magnet synchronous motor drives," IEEE Trans. on Power Electron., vol. 12, no. 3, pp. 528-536, 1997. doi:10.1109/63.575680

[2] Y. P. Liu, "Space Vector Modulated Direct Torque Control for PMSM," Advances in Computer Science, Intelligent System and Environment, Springer, Berlin, Heidelberg, pp. 225-230, 2011. doi:10.1007/978-3-642-23756-0_37

[3] C. Lascua, A. M. Trzynadlowski, "Combining the principles of sliding mode, direct torque control, and space-vector modulation in a high-performance sensorless AC drive," IEEE Transactions on industry applications, vol. 40, no. 1, pp. 170-177, 2004. doi:10.1109/TIA.2003.821667

[4] N. Bekiroglu, S. Ozcira, "Observerless scheme for sensorless speed control of PMSM using direct torque control method with LP filter," Advances in Electrical and Computer Engineering, vol. 10, no. 3, pp. 78-83, 2010. doi:10.4316/AECE.2010.03013

[5] M. M. Rosic, M. Z. Bebic, "Analysis of torque ripple reduction in induction motor DTC drive with multiple voltage vectors," Advances in Electrical and Computer Engineering, vol. 15, no. 1, pp. 105-114, 2015. doi:10.4316/AECE.2015.01015

[6] P. Brandštetter, I. Neborak, M. Kuchař, "Analysis of steady-state error in torque current component control of PMSM drive," Advances in Electrical and Computer Engineering, vol. 17, no. 2, 2017. doi:10.4316/AECE.2017.02006

[7] J. Yu, Y. Ma, H. Yu, C. Lin, "Reduced-order observer-based adaptive fuzzy tracking control for chaotic permanent magnet synchronous motors," Neurocomputing, vol. 214, pp. 201-209, 2016. doi:10.1016/j.neucom.2016.05.088

[8] W. Chang, S. Tong, "Adaptive fuzzy tracking control design for permanent magnet synchronous motors with output constraint," Nonlinear Dynamics, vol. 87, no. 1, pp. 291–302, 2017. doi:10.1007/s11071-016-3043-3

[9] H. Chaoui, P. Sicard, "Adaptive fuzzy logic control of permanent magnet synchronous machines with nonlinear friction," IEEE Transactions on Industrial Electronics, vol. 59, no. 2, pp. 1123-1133, 2011. doi:10.1109/TIE.2011.2148678

[10] Sung-Hoon Yu, Hyo Seok Kang, Yong-Tae Kim, Chang-Ho Hyun, Mignon Park, "Fuzzy adaptive modular design of uncertain chaotic duffing oscillators," International Journal of Control, Automation, and Systems, vol. 12, no. 1, pp. 188-194, 2014. doi:10.1007/s12555-012-0448-8

[11] Dong W. Kim, Ty A. Lasky, Steven A. Velinsky, "Autonomous multi-mobile robot system: simulation and implementation using fuzzy logic," International Journal of Control, Automation, and Systems, vol. 11, no. 3, pp.545-554, 2013. doi:10.1007/s12555-012-0096-z

[12] A. Saidi, F. Naceri, L. Youb, M. Cernat, L. G. Pesquer, "Two types of fuzzy logic controllers for the speed control of the doubly-fed induction machine," Advances in Electrical and Computer Engineering, vol. 20, no. 3, pp. 65-74, 2020. doi:10.4316/AECE.2020.03008

[13] H. K. Lam, Li Hongyi, C. Deters, E. L. Secco, H. A. Wurdemann, K. Althoefer, "Control design for interval type-2 fuzzy systems under imperfect premise matching," IEEE Transactions on Industrial Electronics, vol. 61, no. 2, pp. 956-968, 2014. doi:10.1109/TIE.2013.2253064

[14] E. Yesil, "Interval type-2 fuzzy PID load frequency controller using Big Bang–Big Crunch optimization," Applied Soft Computing, vol. 15, no. 2,pp. 100-112, 2014. doi:10.1016/j.asoc.2013.10.031

[15] E. Kayacan, O. Cigdem, O. Kaynak, "Sliding mode control approach for online learning as applied to type-2 fuzzy neural networks and its experimental evaluation," IEEE Trans. Ind. Electron., vol. 59, no. 9, pp. 3510-3520, 2012. doi:10.1109/TIE.2011.2182017

[16] Hongyi Li, Jiahui Wang, Hak-Keung Lam, Qi Zhou, Haiping Du, "Adaptive sliding mode control for interval type-2 fuzzy systems," IEEE Transactions on Systems, Man, and Cybernetics: Systems, vol. 46, no. 12, pp. 1654-1663, 2016. doi:10.1109/TSMC.2016.2531676

[17] C. S. Lee, M. H. Wang, H. Hagras, "A type-2 fuzzy ontology and its application to personal diabetic-diet recommendation," IEEE Trans. Fuzzy Syst., vol. 18, no. 2, pp. 374-395, 2010. doi:10.1109/TFUZZ.2010.2042454

[18] M. A. Khanesar, E. Kayacan, M. Teshnehlab, O. Kaynak, "Analysis of the noise reduction property of type-2 fuzzy logic system using a novel type-2 membership function," IEEE Trans. Syst., Man, Cybern. B, Cybern., vol. 41, no. 5, pp. 1395-1406, 2011. doi:10.1109/TSMCB.2011.2148173

[19] P. Z. Lin, C. M. Lin, C. F. Hsu, T. T. Lee, "Type-2 fuzzy controller design using a sliding-mode approach for application to DC–DC converters," IEE Proc.-Electr. Power Appl., vol. 152, no. 6, pp. 1482-1488, 2005. doi:10.1049/ip-epa:20045232

[20] M.H. Khooban, N. Vafamand, A. Liaghat, T. Dragicevic, "An optimal general type-2 fuzzy controller for urban traffic network," ISA Transactions, vol. 66, no. 1, pp. 335-343, 2017. doi:10.1016/j.isatra.2016.10.011

[21] X. Lu, Y. Zhao, M. Liu, "Self-learning interval type-2 fuzzy neural network controllers for trajectory control of a Delta parallel robot," Neurocomputing, vol. 283, pp. 107-119, 2018. doi:10.1016/j.neucom.2017.12.043

[22] M. A. Sanchez, O. Castillo, J. R.Castro, "Generalized Type-2 Fuzzy Systems for controlling a mobile robot and a performance comparison with interval type-2 and type-1 fuzzy systems," Expert Systems with Applications, vol. 42, no. 14, pp. 5904-5914, 2015. doi:10.1016/j.eswa.2015.03.024

[23] F. J. Lin, P. H. Shieh, Y. C. Hung, "An intelligent control for linear ultrasonic motor using interval type-2 fuzzy neural network," IET Electr. Power Appl., vol. 2, no. 1, pp. 32-41, 2008. doi:10.1049/iet-epa:20070060

[24] F. J. Lin, P. H. Chou, P. H. Shieh, S. Y. Chen, "Robust control of an LUSM-based X–Y–θ motion control stage using an adaptive interval type-2 fuzzy neural network," IEEE Trans. Fuzzy Syst., vol. 17, no. 1, pp. 24-38, 2009. doi:10.1109/TFUZZ.2008.2005938

[25] F. J. Lin, P. H. Chou, "Adaptive control of two-axis motion control system using interval type-2 fuzzy neural network," IEEE Trans. Ind. Electron., vol. 56, no. 1, pp. 178-193, 2009. doi:10.1109/TIE.2008.927225

[26] S. Barkat, A. Tlemçani, H. Nouri, "Non-interacting adaptive control of PMSM using interval type-2 fuzzy logic systems," IEEE Trans. Fuzzy Systems, vol. 19, no. 5, pp. 925-936, 2011. doi:10.1109/TFUZZ.2011.2152815

[27] S. Masumpoor, H. Yaghobi, M. A. Khanesar, "Adaptive sliding-mode type-2 neuro-fuzzy control of an induction motor," Expert Systems with Applications, vol. 42, no. 19, pp. 6635-6647, 2015. doi:10.1016/j.eswa.2015.04.046

[28] H. Chaoui , M. Khayamy, A. A. Aljarboua, "Adaptive interval type-2 fuzzy logic control for PMSM drives with a modified reference frame," IEEE Transactions on Industrial Electronics, vol. 64, no. 5, pp. 3786 – 3797, 2017. doi:10.1109/TIE.2017.2650858

[29] Q. Liang, J. M. Mendel, "An introduction to type-2 TSK fuzzy logic systems," IEEE International Fuzzy Systems Conference, Seoul, Korea, pp. 1534-1539, 1999. doi:10.1109/FUZZY.1999.790132

[30] N. N. Karnik, J. M. Mendel, Q. Liang, "Type-2 fuzzy logic systems," IEEE Trans. Fuzzy Syst., vol. 7, no. 6, pp. 643-658, 1999. doi:10.1109/91.811231

[31] A. Tlemçani, O. Bouchhida, K. Benmansour, D. Boudana, M. S. Boucherit, "Direct torque control strategy (DTC) based on fuzzy logic controller for a permanent magnet synchronous machine drive," Journal of Electrical Engineering & Technology, vol. 4, no. 1, pp. 66-78, 2009. doi:10.5370/JEET.2009.4.1.066

[32] H. K. Lam, L. D. Seneviratne, "Stability analysis of interval type-2 fuzzy-model-based control systems," IEEE Trans. Syst., Man, Cybern. B, Cybern., vol. 38, no. 3, pp. 617-628, 2008. doi:10.1109/TSMCB.2008.915530

[33] M. Biglarbegian, W. W. Melek, J. M. Mendel, "On the stability of interval type-2 TSK fuzzy logic control systems," IEEE Trans. Syst., Man, Cybern. B, Cybern., vol. 40, no. 3, pp. 798-818, 2010. doi:10.1109/TSMCB.2009.2029986